Spatial Dynamics Evolution of Land use for the Study of the Local Traditional Living Changes

Arunplod, C.,[1] Phonphan, W.,[2*] Wongsongja, N.,[2] Utarasakul, T.,[2] Niemmanee, T.,[2] Daraneesrisuk, J.[3] and Thongdara, R.[4]

[1]Department of Geography, Faculty of Social Sciences, Srinakharinwirot University, Watthana, Bangkok, Thailand, E-mail: chomchanok@g.swu.ac.th

[2]Faculty of Sciences and Technology, Suan Sunandha Rajabhat University, Dusit, Bangkok, Thailand E-mail: walaiporn.ph@ssru.ac.th,* nich.wo@ssru.ac.th, tatsanawalai.ut@ssru.ac.th, talisa.ni@ssru.ac.th

[3]Remote Sensing and GIS (FoS), School of Engineering and Technology, Asian Institute of Technology Klong Luang, Pathum Thani, Thailand, E-mail: jirawatdns@gmail.com

[4]Department of Civil and Environmental Engineering, Mahidol University, Salaya, Nakhon Pathom, Thailand E-mail: romanee.tho@mahidol.ac.th

Corresponding Author

DOI: https://doi.org/10.52939/ijg.v19i4.2635

Abstract

Land use data can be used to understand patterns of economic behavior, such as the relationship between land use and property values or the impact of land use on environmental factors like air and water quality. The combination of land use data with other data sources and analysis methods can yield significant insights into economic growth and behavior. In this study, the land use and land cover (LULC) were classified using multi-temporal Sentinel-2 imagery (2019 and 2021) and random forest through the Google Earth Engine platform (GGE) with an overall accuracy of more than 89.79%. According to the results of the change detection analysis, there was a 16.96% increase in miscellaneous surface areas and a 15.50% increase in artificial surface areas. These disclose confirm that the sea salt farm, which are the traditional economic function, are losing 37.40%. Furthermore, the CA-Markov model was utilized to predict alterations in land use patterns in the year 2023 through the extrapolation of existing trends. The predicted LULC map of 2023 publicizes the trend of the sea salt farm decreasing, contrasty the artificial surface areas are increasing. In summary, this research reveals the evidence that LULC is strongly related to traditional living changes, and spatial analysis techniques are reasonable and committing tools for study.

Keywords: CA-Markov, Google Earth Engine, LULC, Multi-temporal, Sentinel-2

1. Introduction

Human activities reflect land use in the way how people use the land for a specific purpose. Humans need the land for living, and they notice the house on the land. Therefore, land use data can be used to understand economic growth and behavior. Land use data provides information about how land is being used, such as whether it is being used for agriculture, industry, or residential purposes, and this can be used to analyze economic activity in those areas. For example, an increase in land use for industrial purposes may indicate growth in the manufacturing sector and suggest a growing local economy. Alternatively, a decrease in land use for agriculture may indicate a shift away from traditional farming practices and towards other economic activities, such as tourism or services [1]. Land use data can also be used to understand patterns of economic behavior, such as the relationship between land use and property values or the impact of land use on environmental factors like air and water quality. Understanding these relationships can inform policy decisions and guide investments in infrastructure and development. Overall, land use data can be a valuable tool for understanding economic growth and behavior [2] and [3], particularly when combined with other data sources and analysis methods. To be achieved this, the land activities that change over time have to investigate [4] [5] [6] and [7]. Land use and land cover (LULC) mapping derived from satellite imagery is a valuable source of information that offers current insights into various stages of transformation occurring on the Earth's surface [8].

In addition, the time series of imagery allows a seasoning of landscape and actual processes such as urban expansion, crop rotation, and deforestation [9]. Besides, the procedure of land's surface can be detected or computed with satellite imagery through a multi-temporal perspective [10]. As a result, remote sensing has emerged as the most effective and reliable method for characterizing and analyzing land-use and land-cover conditions and changes, and its usage has increased significantly over time [11]. The Sentinel-2 satellites equipped with multispectral imaging instruments (MSI) offer high-resolution satellite data that is useful for monitoring LULC [12]. This missions are aimed at ensuring continuity and improving upon the accomplishments of the Landsat missions [13].

Presently, the widely usage tool for satellite data accesses and processes is the Google Earth Engine (GEE). The GEE is a cloud-based computing platform that is easily accessible and capable of storing and processing large-scale geospatial data in the petabyte range. There is easily accessible and user-friendly with interactive data and processing algorithms [14]. Also, GEE provides high performance of cloud computation and multiple practical tools for carrying out the analysis of global geospatial big data. Currently, it is widely acknowledged as the most popular cloud computing platform in the fields of Earth and Environmental Science [15] that is commonly utilized for processing data related to various fields focused on environmental change, such as crop analysis [16], water resources [17], land cover mapping [18], disaster monitoring [19], climate change [20], soil properties [21], forest [22] and urbanization [23]. Due to the inability of traditional computing resources to handle multi-time series satellite images over large areas, the GEE service has emerged as an effective platform for supporting the analysis of global and regional land changes [24].

In this research, the LULC classification was conducted using the Sentinel-2 time-series imagery in conjunction with the random forest algorithm on the GEE platform. In addition, we conducted a change detection analysis to examine the LULC changes in Phetchaburi and Samut Songkhram provinces between the years 2019 and 2021. The cellular automata - Markov chain model (CA–Markov) deployed in the TerrSet software developed by Clark (formerly IDRISI), with the high reputation and widely acceptation. The software provides an excellent advantage and essential geospatial tools for the study of land-cover changes and probable prediction [25]. This study, itis used to predict the possible LULC in 2023. Additionally, the objectives of our study included the classification of LULC using a sustainable cloud-computing platform and training dataset, as well as the simulation of future land cover changes in our study area located in western Thailand through the utilization of the CA-Markov model.

2. Materials

2.1 Study Area

This research sites are located in Phetchaburi and Samut Songkhram provinces (Figure 1). These provinces are in the western region of Thailand (12°33′45″N to13°31′7″ N and 100°6′12″E to 99°6′2″ E) and cover the area of 6585.28 km^2. The natural border between Thailand and Myanmar is formed by the presence of high mountains and forests in the western region. Also, the east site is a coastline be a part of the gulf of Thailand. In addition, the Kaeng Krachan National Park, which was declared as a potential UNESCO Natural World Heritage site in 2013, is located in the western region [26].

2.2 Background of Study Site

The Phetchaburi province has a forestry of 57.24%, an agricultural area of 28.86%, and a build-up of 5.14%. The total population is approximately 480,000 people and the gross provincial product (GPP) was about 63,000 million bath and the GPP per capita was about 130,000 baht/year in 2016. The largest economic value about 37,000 million baht which contributed by the industrial sector and the agriculture sector. Primary economic activities in Phetchaburi is salt producer and horticulture such a palm sugar, rose apple, and etc.

The Samut Songkhram province has an agricultural area of 68.22%, a build-up of 15.24%, and forestry of 6.79%. The total population was approximately 194,000 people and the gross provincial product (GPP) was 20,400 million baht and GPP per capita was 105,000 baht/year in 2016 as well. Primary economic activity worth 12,600 million bahtwhich contributed by the agriculture sector, fishery, and tourist. The Samut Songkhram is known as salt producer as well as the Phetchaburi. Additional, the horticulture and fishery are also prime contributes in economic activities.

The main economic sectors in those area are the agriculture, fishery, and sea salt farm. The rapid expansion of industrial area in last decade is the most driving force to change the traditional economic sectors to industrial sectors which reflecting on land use change, as well as the local traditional living.

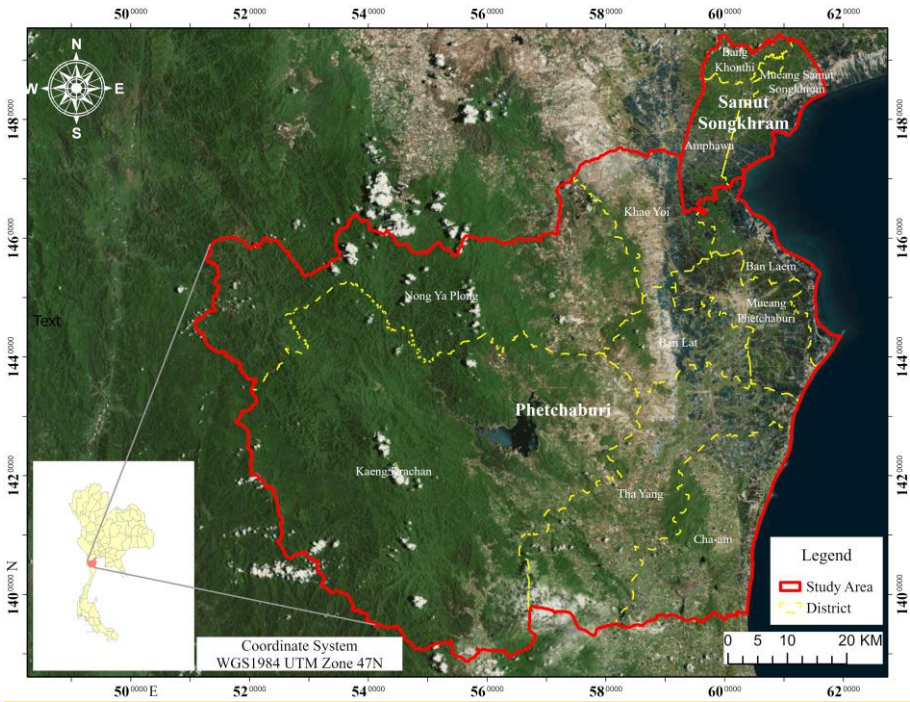

Figure 1: The study area of Phetchaburi and Samut Songkhram provinces

2.3 Dataset

The data used in this study are composed of two historic Sentinel-2 satellite imagery (2019 and 2021) with a spatial resolution of 10-meter. The imagery scenes that covered the study area irrespective of cloud cover were operated in the GEE platform. The image datasets were already geo-referenced, projected, and provided the atmospheric corrections. In addition, the land use datasets of Phetchaburi and Samut Songkhram province from the Land Development Department (LDD) were used to perform the training dataset for machine learning classification. These datasets were produced by visual interpretation from LULC experts of government. Also, the study area's ground truth dataset was observed randomly and covered in different LULC classes. The identified LULC classes were compared and matched with similar types observed in both the classified imagery and training dataset. Moreover, the independent variable datasets were collected to support the prediction model: the digital elevation model (DEM), the road network dataset, the stream dataset, and the land use dataset.

3. Methodology

In this section, we describe the major anticipated uses for the LULC changes in the future. The time-series raster dataset from Sentinel-2 imagery was classified using a machine learning algorithm on the Google Earth Engine platform. The primary workflow implemented in this study involved: (1) the mapping of 2019 and 2021 using the random forest classifier of satellite imagery, (2) an analysis of change detection, (3) predicting LULC changes using a CA-Markov Model in the year 2023 was a crucial aspect of the workflow in this study. The overall workflow illustrates in Figure 2.

3.1 Data Preparation

The time-series Sentinel-2 images were used in 2019 and 2021. Sentinel-2 (L2A) products were used in this study, which is corrected reflectance products [27] and [28], and are available on GEE. Cloud cover is a significant limiting factor in time-series datasets from satellite sensors, particularly in rainforest regions [29]. Hence, the library of sentinel-2 cloud probability product was utilized on the GEE platform to mask the cloud cover in all sentinel-2 images. We separate the period of imagery into three periods of each year: a beginning period (January-April), a middle period (May-August), and the end period (September-December). Each period consisted of five generated bands, namely; Blue, Green, Red, NIR, SWIR, and three indices named as NDVI, NDWI, and NDBI, that were resampled into 10-meter pixel sizes of all bands as demonstrates in Figure 3.

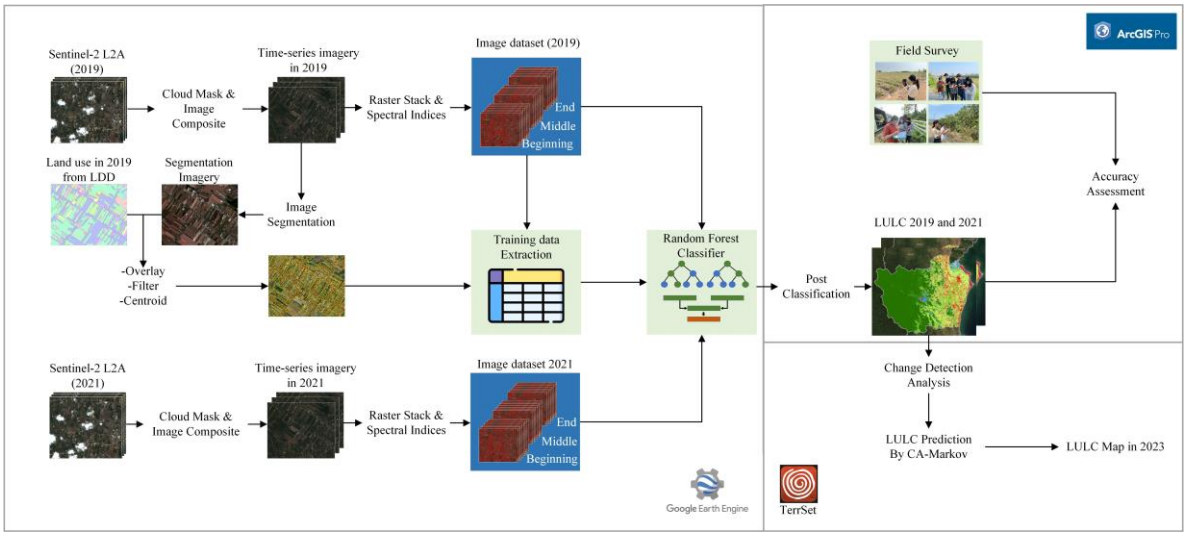

Figure 2: Overall methodology

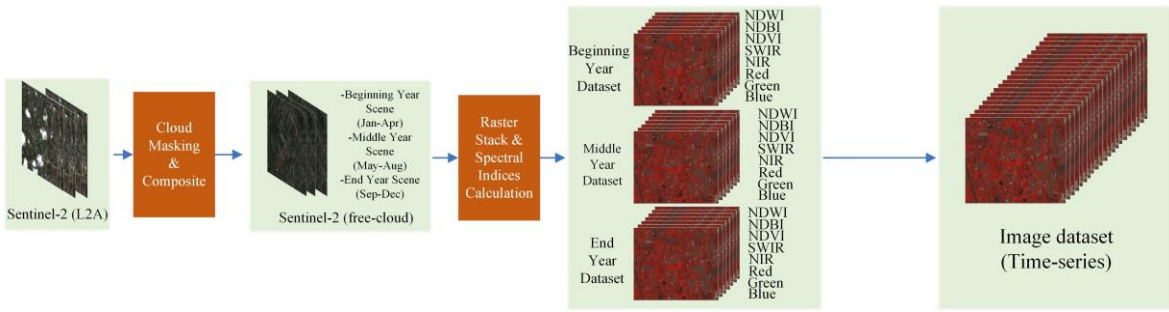

Figure 3: Image composite approach in this study

The landuse dataset from Thailand's Land Development Department (LDD) in 2019 was used to generate the training dataset. First, we group LULC classes from the LDD landuse dataset into 11 categories which are applied based on The System of Environmental-Economic Accounting (SEEA) of the United Nations [30].The LULC classes are modified based on the eight traditional found in study area therefore, included: artificial surfaces (AS), herbaceous crops (HC), woody crops (WC), tree-covered areas (TC), mangroves (MG), water bodies (WB), salt fields (SF) and miscellaneous (MC), representing of geographic areas dominated by natural cover, the detailed of description publicize in Table 1. Also, we select the image of the beginning period of 2019 to generate image segmentation using the GEE platform and convert it to a vector dataset. Next, the landuse dataset and segmentation dataset in the form of vector data overlay into the dataset. Then, we perform the centroid of all polygon features representing the training location of LULC in this study. After, the centroid datasets were operated with Sentinel-2 images in 2019 to obtain the training dataset of 21 values in each centroid (five bands and three indices in three-period each).

3.2 Image Classification

We classified the LULC classes from Sentinel-2 imagery in 2019 and 2021 with the predictor variables associated with land cover for each location in the training data of 2019. After preparing the training data, we used it to predict all eight-LULC classes in Sentinel-2 imagery for the years 2019 and 2021. The land cover classification was carried out using a random forest classifier, which is one of the most commonly used classifiers for image classification based on remotely sensing data [31]. This classifier mothed has received considerable interest over the last two decades: its good handling of the outliers and noisier datasets, good performance with multi-dimension and sources datasets, and higher accuracy than other algorithms [32]. The final LULC map in 2019 and 2021 of Phetchaburi and Samut Songkhram province were produced.

Table 1: The LULC classes in this study

Previous LULC based on SEEA	LULC reclassify in this study	Description
Artificial surface	Artificial surface (AS)	This class is composed of artificial surfaces, including urban and associated areas, for example, urban buildings, concrete parks, industrial areas, and waste dump deposits.
Herbaceous crop	Herbaceous crop (HC)	This land cover class includes cultivated herbaceous plants such as non-perennial crops that do not survive for more than two growing seasons. Also, this class includes cultivated herbaceous plants, such as non-perennial crops that have a lifespan of two growing seasons or less. These crops are typically harvested for their upper parts, while the root systems can persist for over a year. Examples of such crops include sugarcane, paddy, and maize.
Woody crops	Woody crops (WC)	This class consists of permanent crops, including orchards and plantations that are not cut for harvested purposes. Examples include fruit trees, coffee and tea plantations, oil palms, and rubber plantations.
Tree-covered areas	Tree-covered areas (TC)	This class is any geographic area covered by more than 10% of natural tree plants, shrubs, and herbs that are density higher than trees. Also, the trees for afforestation and forest plantation are included.
Mangroves	Mangroves (MG)	This class encompasses any geographic area where woody vegetation covers more than 10% of the land and is consistently or periodically flooded by salt and brackish water.
Water bodies	Water bodies (WB)	This class includes any geographic area that is covered by inland water bodies for the majority of the year.
Salt fields	Salt fields (SF)	This class is about any area covered a salt from human activities.
Grassland	Miscellaneous (MC)	This class includes geographic areas dominated by natural herbaceous plants, shrubs, and vegetation, covering less than 10% of the area.
Shrub-covered area		
Sparsely natural vegetation areas		
Terrestrial barren land		

3.3 Accuracy Assessment

Popular measures extracted from confusion matrix reports, such as overall accuracy, producer accuracy, and user accuracy were used [34]. This process is important in determining image classification method that provides reliability and accuracy [35]. The field survey in March 2022, which is nearby image classified, was performed to collect the actual ground points covered in all classes of LULC. The equation is as follow:

$$OA = \left[\frac{Pc + Nc}{Pc + Fp + Nc + Fn} \right] \times 100$$

Equation 1

Where:

OA or Overall Accuracy = the percentage of correctly classified pixels in the entire image or area.

Pc or Producer's Accuracy = the proportion of actual positive pixels correctly identified or classified by the model.

Nc or User's Accuracy = the proportion of actual negative pixels correctly identified or classified by the model.

Fp or False Positive Rate = the number of negative pixels classified as positive incorrectly.

Fn or False Negative Rate = the number of positive pixels incorrectly classified as negative.

3.4 Land Change Modeler (LCM)

The results of the LULC classification in 2019 and 2021 were employed in the RECLASS module of the software [36]. All values, including background values (-9999), were reclassified as class 0 to background values, class 1 to artificial surfaces, class 2 to herbaceous crops, class 3 to woody crops, class 4 to tree-covered areas, class 5 to mangroves, class 6 to water bodies, class 7 to salt fields, and class 8 to miscellaneous areas. For analyzing the change in LULC, we conducted a change analysis by comparing the differences between the LULC of 2019 and 2021.

3.5 CA-Markov Model

One of the most efficient models in current LULC modeling tools is the CA-Markov model. The CA-Markov model is a practical tool that combines Markov and Cellular automata (CA) approaches to simulate land use changes. It is important to consider both time series and spatial data when forecasting and modeling land use changes, as this can help to better simulate the temporal and spatial patterns of these changes [37]. Markov probability is utilized to predict the future state of a system based on its present state, without considering the past states. Cellular automata, on the other hand, is a model derived from the fields of physics and biology, which uses a natural mechanism to simulate and comprehend complex behaviors [38]. We employed the integrated CA-Markov approach to predict future land use changes based on the 2019 and 2021 datasets. To achieve this, we prepared the transition probability matrix (TPM), transition probability area (TPA), and transition suitability image (TSI) using the Markov model. These outputs were then used in the CA-Markov model.

4. Results and Discussion

4.1 LULC Classification and Changing

The present study utilized Sentinel-2 time series data from 2019 and 2021 to perform LULC classification through the random forest classifier of the machine learning approach. The classification accuracy was evaluated using a confusion matrix and ground truth data obtained from field surveys. The overall accuracy of the classification was found to be 87.79%. Table 2 shows that the highest classification accuracy was obtained for water bodies (WB), salt fields (SF), and artificial surfaces (AS), respectively. It was found that separating salt fields from paddy fields or construction sites posed a challenging issue due to similarities in geometry, however, spectral classification based on the presence of even thin layers of salt was found to be useful. Furthermore, due to the limitations of the spatial resolution of the image, small artificial objects were difficult to extract, and therefore, grouping pixel technique was applied to enhance the limitations of this issue.

Overall, LULC change between 2019 and 2021, in addition to Table 3**,** revealed an increasing trend in human-made structures and tree plants, whereas the land for local economic functions such as HC, WC, and SF, showed a decreasing trend. Even the agricultural map, Agri-map, reported by the Land Development Department (LDD) in 2021, recommended the transformation of herbaceous plants to GI's plantation including lychee, coconut, and pomelo since 2019, following appropriate agricultural extension guidelines [39].

Table 2: Accuracy assessment of classified LULC in 2021

LULC Class		Ground Reference data								Total	UA
		AS	HC	WC	TC	MG	WB	SF	MC		
Classified	AS	344							3	347	99.14
	HC	20	162				10			192	84.38
	WC	4	30	129						163	79.14
	TC			8	28				2	38	73.68
	MG				2	5				7	71.43
	WB						102			102	100.00
	SF							20		20	100.00
	MC			1	46				116	163	71.17
Total		368	192	138	76	5	112	20	121	1032	
PA		93.48	84.38	93.48	36.84	100	91.07	100	95.87	**OA = 87.79%**	

Table 3: The LULC changes observed between 2019 and 2021

LULC Class	2019		2021	
	Area (sq.km.)	Percent (%)	Area (sq.km.)	Percent (%)
1. Artificial surface (AS)	515.6	7.8	610.2	9.3
2. Herbaceous crops (HC)	1,222.9	18.6	1,060.7	16.1
3. Woody crops (WC)	686.2	10.4	622.8	9.5
4. Tree-covered areas (TC)	3,581.9	54.4	3,680.2	55.9
5. Mangroves (MG)	56.1	0.9	51.8	0.8
6. Water bodies (WB)	323.7	4.9	343.6	5.2
7. Salt fields (SF)	50.4	0.8	36.7	0.6
8. Miscellaneous (MC)	151.2	2.3	182.1	2.8
Total	**6,588.0**	**100.0**	**6,588.0**	**100.0**

Figure 4: Results of LULC change between 2019 and 2021;
(a) gain and loss of LULC, (b) overall net change in all LULC categories,
(c) artificial surface, (d) herbaceous crops, (e) woody crops, (f) tree-covered areas, (g) mangroves,
(h) water bodies, (i) salt fields, and (j) miscellaneous

In contrast, Phetchaburi is renowned for its production of high-quality sea salt, key limes, palm sugar, rose apples, pineapples, and bananas, among other items [40]. However, the traditional yield has experienced a drastic decline due to a reduction in manpower in those sectors. The Land Change Modeler (LCM) available in the software was utilized to conduct a detailed investigation of the LULC changes from 2019 to 2021. The LCM generated a grain and loss chart, depicted in Figure 4, which represents the way LULC classes transition from one to another.

The HC class was found to be decreasing from 2019 to 2021, with a conversion to WC of approximately 40 km^2, as seen in Figure 4(d) and 4(e). This indicates a shift in the main economic activity, with the promotion of fruit tree plantations gradually gaining momentum in this area. Additionally, the WB areas increased by around 12.5 km^2, which is the highest change from SF. This provides evidence that the salt fields are being abandoned or converted into other land utilities, as shown in Figure 4(h) and 4(i). The most significant change observed was in the artificial surface (AS), which increased by almost 60 km^2, primarily constructed or converted from HC, as depicted in Figure 4. This LULC analysis revealed that HC experienced the most significant changes among other classes due to the continued decline of herbaceous crops' economic function in this area. In addition to its rich cultural heritage and agricultural productivity, Phetchaburi has become a popular tourist destination due to its unique topography. As depicted in Figure 5, the number of tourist accommodations has been steadily increasing since the Tourism Authority of Thailand (TAT) tourism campaign in 2017, indicating a growing demand for tourism-related activities in the region. Furthermore, the urban expansion in the area is reflected in the increasing presence of artificial surfaces, such as roads and highways, as seen in Figure 5. This expansion has led to an extension of the transportation network, facilitating the movement of people and goods within and beyond the region.

The spatial resolution of remote sensing images plays a crucial role in accurate Land Use and Land Cover (LULC) classification. However, it has been observed that a 10-meter resolution image can significantly impact the classification results, particularly in the case of objects with intricate details, such as trees and small buildings/constructions. In addition, the limited spatial resolution often leads to a mixture of spectral reflectance values, resulting in the extraction of erroneous information and confusion in near-character objects. Therefore, caution must be exercised while selecting the appropriate spatial resolution for the remote sensing image to ensure the accuracy and reliability of the LULC classification results.

4.2 The LULC Simulation in 2023

LULC change extraction is a magnificent tool for economic and urban behaviors; therefore, LULC simulation in 2023 is applied for LULC change prediction. The map of LULC change in this study from 2019 and 2021 was initial as the dependent variable to perform the MLP neural network, preparing as two classes, namely: No change and LULC change, as shown in Figure 6a.

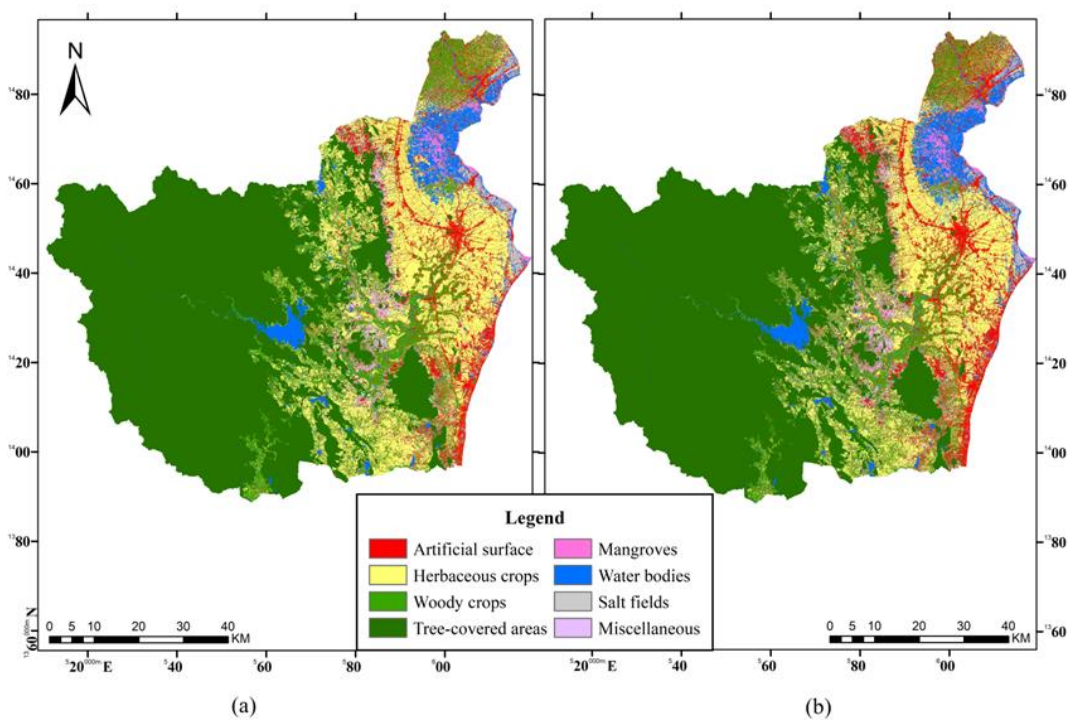

Figure 5: The LULC classifications (a) 2019, and (b) 2021

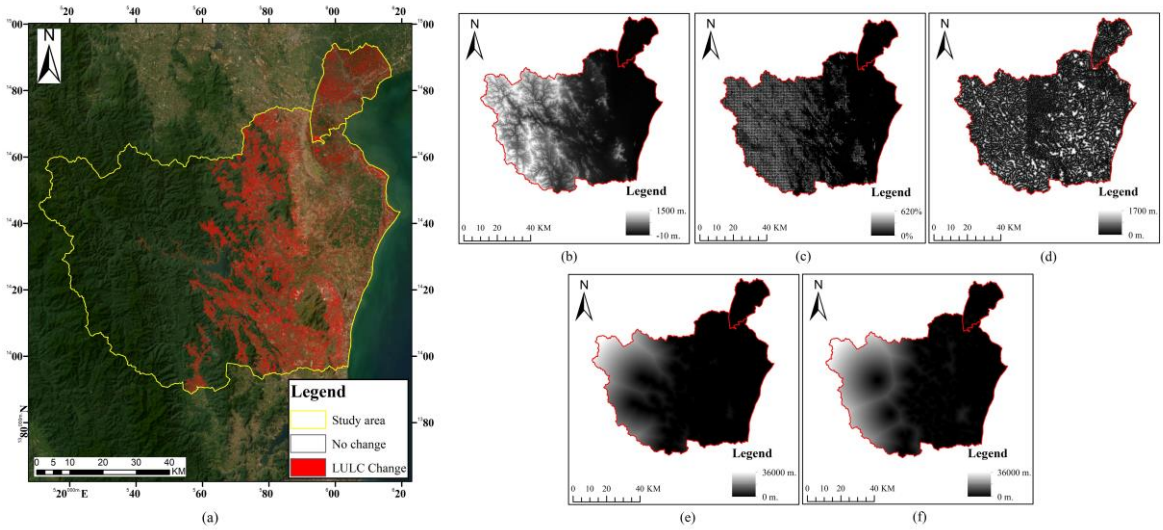

Figure 6: LULC change analysis results (a) ULC Change from 2019 to 2021, (b) elevation, (c) slope, (d) distance to stream, (e) distance to road, and (f) distance to urban and village

Table 4: Sub-modules and Cramer's V value for simulation

LULC	Factor				
	Elevation	**Slope**	**Distance to stream**	**Distance to road**	**Distance to urban and village**
Overall V	**0.3336**	**0.0092**	**0.0097**	**0.2191**	**0.2582**
1. Artificial surface	0.0000	0.0000	0.0000	0.0000	0.0000
2. Herbaceous crops	0.3700	0.0038	0.0107	0.2243	0.2653
3. Woody crops	0.4497	0.0091	0.0155	0.3075	0.3650
4. Tree-covered areas	0.3050	0.0038	0.0015	0.2259	0.2630
5. Mangroves	0.8755	0.0015	0.0200	0.6198	0.7303
6. Water bodies	0.1427	0.0204	0.0041	0.0621	0.0734
7. Salt fields	0.2650	0.0120	0.0049	0.1571	0.1863
8. Miscellaneous	0.1200	0.0031	0.0035	0.0525	0.0635

Table 5: The transition probability matrix for LULC change

LULC Class	**Prediction**							
	AS	**HC**	**WC**	**TC**	**MG**	**WB**	**SF**	**MC**
AS	1.000	0.0000	0.0000	0.0000	0.0000	0.0000	0.0000	0.0000
HC	0.0482	0.7625	0.1074	0.0319	0.0019	0.0180	0.0002	0.0299
WC	0.0313	0.1271	0.6256	0.1098	0.0107	0.0049	0.0000	0.0906
TC	0.0004	0.0034	0.0107	0.9778	0.0004	0.0003	0.0000	0.0071
MG	0.0180	0.0595	0.1423	0.0229	0.6688	0.0852	0.0013	0.0020
WB	0.0130	0.0392	0.0048	0.0030	0.0113	0.9101	0.0179	0.0007
SF	0.0217	0.0113	0.0000	0.0000	0.0033	0.3579	0.6058	0.0000
MC	0.0476	0.1225	0.2267	0.1307	0.0008	0.0028	0.0000	0.4688

The model utilized five driving factors or variables: elevation, slope, distance to stream, distance to road, and distance to urban and village areas, as shown in Figure. 6b – 6f. The dominant factors were calculated using Cramar's V values, which determining the most dominant factor in LULC change is elevation and distance to urban and village as shown in Table 4.

Associated with the driving factor, a Markov chain analysis was used to produce the changing dynamic of the LULC classes. The transition probability matrix (TPM) was generated to forecast the future patterns of LULC and the results presented in Table 5. Based on human behavior, they were unlikely to return to tree cover or other land uses once artificial surfaces were established.

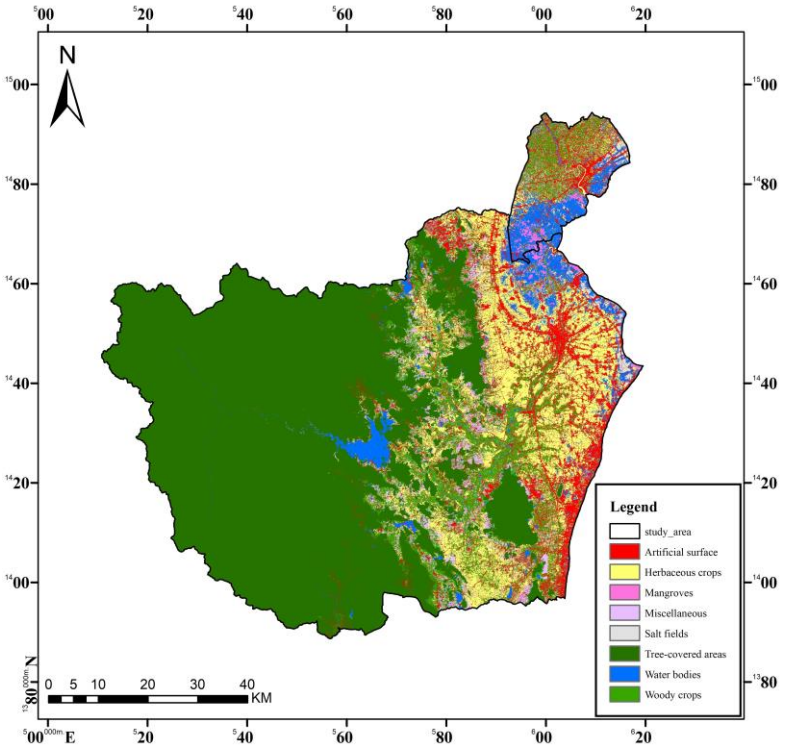

Figure 7: The LULC prediction in 2023

Table 6: The comparison of LULC change between 2019, 2021, and 2023

LULC Class	2019	2021	2023
	Area (sq.km.)	Area (sq.km.)	Area (sq.km.)
1. Artificial surface	515.6	610.2	697.10
2. Herbaceous crops	1,222.9	1,060.7	939.70
3. Woody crops	686.2	622.8	593.22
4. Tree-covered areas	3,581.9	3,680.2	3,726.36
5. Mangroves	56.1	51.8	48.92
6. Water bodies	323.7	343.6	354.03
7. Salt fields	50.4	36.7	28.63
8. Miscellaneous	151.2	182.1	200.01
Total	**6,588.0**	**6,588.0**	**6,588.0**

Therefore, it was predicted that the current artificial surface (AS) would remain as the AS in 2023 with a probability of 100%, as shown in Table 5. Additionally, the study found a high probability of no change in the tree cover (TC) class, which may be attributed to most TC areas belonging to national forest parks. The change of LULC between 2019 and 2021 yields the LULC in 2023, Figure 7, demonstrating that artificial surface (AS) was the dominant change in this area (Table 6). The predicted AS in 2023 is distributed in tree-covered areas, nearby the dam in the forest area, a water body illustrated in the center of the map, and along a shoreline in the right part of the map in Figure 7 as well. The prediction of AS aligns with the government promoting plan that the recent acceptance of Phetchaburi into the UNESCO Creative Cities Network (UCCN) for gastronomy in 2021, as well as the growing demand for tourist activities due to the post-COVID-19 pandemic, has led to an increase in tourist facilities and construction, which were found through remote investigation to be associated with the next normal paradigm. However, during 2019 – 2021, the COVID-19 pandemic had a profound impact on society and the economy worldwide and affected the availability and quality of data. Data collection during the pandemic may have been more challenging due to restrictions on movement and face-to-face interactions. As a result, there may have been gaps or biases in the data that were collected, which could have affected the accuracy of the research findings.

The next normal paradigm is mentioned in post-pandemic affected different aspects of social and economic life, including changes in behavior, mobility patterns, and consumption patterns. These changes could have affected the land use patterns and economic activities that were being studied.

5. Conclusion

In conclusion, this study has successfully classified land use and land cover (LULC) using the internationally recognized System of Environmental-Economic Accounting (SEEA) standard and has utilized a cellular automata-Markov chain (CA-Markov) model to predict future LULC in Phetchaburi and Samut Songkhram provinces, Thailand. The random forest algorithm applied to the Sentinel-2 time-series imagery yielded an overall accuracy of approximately 87%, and the model closely matched LULC types with field observations. The LULC change analysis conducted between 2019 and 2021 revealed significant changes in the spatial and quantitative distribution of LULC. Notably, the study found a slight increase in artificial surfaces, tree-covered water bodies, and miscellaneous areas, while herbaceous crops, woody crops, mangroves, and salt field areas decreased significantly during the same period. Additionally, the study demonstrated the potential for LULC to explain socioeconomic patterns in a target area when associated with economic data. Access to various datasets is essential for informing land use and land cover planning decisions to promote environmental sustainability. The limitations of Sentinel-2 imagery, which does not provide historical imagery over several decades, are acknowledged. However, the continuous operation of the product in high resolution similar to Landsat provides opportunities for future research that can input more time-series imagery and training datasets covering all classes of LULC in multiple regions and countries. Incorporating demographic data into the analysis is critical to understanding the long-term dynamics of LULC change and its implications for achieving sustainable development. These findings make significant contributions to the field of LULC analysis and provide a foundation for future research in sustainable land use management and conservation.

Acknowledgment

The authors express their sincere gratitude for the financial support provided by Suan Sunandha Rajabhat University and the partial financial and fieldwork support provided by the Faculty of Social Science, Srinakharinwirot University, for this research project. Their contributions have been invaluable to the successful completion of this study.

References

[1] Kim, J. H., (2011). Linking Land Use Planning and Regulation to Economic Development: A Literature Review. *Journal of Planning Literature*, Vol. 26(1), 35-47. https://doi.org/ 10.1177/0885412210382985.

[2] He, C., Huang, Z. and Wang, R., (2014). Land Use Change and Economic Growth in Urban China: A Structural Equation Analysis. *Urban Studies*, Vol. 51(13), 2880-2898, https://doi.org/ 10.1177/0042098013513649.

[3] Wentland, S. A., Ancona, Z. H., Bagstad, K. J., Boyd, J., Hass, J. L., Gindelsky, M. and Moulton, J. G., (2020). Accounting for Land in the United States: Integrating Physical Land Cover, Land Use, and Monetary Valuation. *Ecosystem Services*, Vol. 46(3). https://doi.org/ 10.1016/ j.ecoser.2020.101178.

[4] Bruckner, M., Fischer, G., Tramberend, S. and Giljum, S., (2015). Measuring Telecouplings in the Global Land System: A Review and Comparative Evaluation of Land Footprint Accounting Methods. *Ecological Economics*, Vol. 114, 11-21. https://doi.org/10.1016/j. ecolecon.2015.03.008.

[5] Jafarpour Ghalehteimouri, K., Shamsoddini, A., Mousavi, M. N., Binti Che Ros, F. and Khedmatzadeh, A., (2022). Predicting Spatial and Decadal of Land Use and Land Cover Change Using Integrated Cellular Automata Markov Chain Model-Based Scenarios (2019–2049) Zarriné-Rūd River Basin in Iran. *Environmental Challenges*, Vol. 6. https://doi. org/10.1016/j.env c.2021.100399.

[6] Joshi, N., Baumann, M., Ehammer, A., Fensholt, R., Grogan, K., Hostert, P., Jepsen, M. R., Kuemmerle, T., Meyfroidt, P., Mitchard, E. T. A., Reiche, J., Ryan, C. M. and Waske, B., (2016). A Review of the Application of Optical and Radar Remote Sensing Data Fusion to Land Use Mapping and Monitoring. *Remote Sensing*, Vol. 8(1). https://doi.org/10.3390/rs8010070.

[7] Recatalá, L., Ive, J. R., Baird, I. A., Hamilton, N. and Sánchez, J., (2000). Land-use Planning in the Valencian Mediterranean Region: Using LUPIS to Generate Issue Relevant Plans. *Journal of Environmental Management*, Vol. 59(3), 169-184. https://doi.org/10.1006/jema. 2000.0350.

[8] Weigand, M., Staab, J., Wurm, M. and Taubenböck, H., (2020). Spatial and Semantic Effects of LUCAS Samples on Fully Automated Land Use/Land Cover Classification in High-Resolution Sentinel-2 Data. *International Journal of Applied Earth Observation and*

Geoinformation, Vol. 88, 1-9. https://doi.org/10. 1016/j.jag.2020.102065.

[9] ED Chaves, M., CA Picoli, M. and D. Sanches, I., (2020). Recent Applications of Landsat 8/OLI and Sentinel-2/MSI for land Use and Land Cover Mapping: A Systematic Review. *Remote Sensing*, Vol. 12(18), https://doi.org/10.3390/ rs12183062

[10] Carlson, T. N. and Sanchez-Azofeifa, G. A., (1999). Satellite Remote Sensing of Land Use Changes in and around San José, Costa Rica. *Remote Sensing of Environment*, Vol. 70(3), 247-256. https://doi.org/10.1016/S00344257(99) 00018-8.

[11] Phonphan, W. and Thanakunwutthirot, M., (2020). Mapping of Mangrove Change with Remote Sensing in Samut Songkhram Province, Thailand. *Human Interaction, Emerging Technologies and Future Applications II, Cham, April 23-25, 2020*, T. Ahram, R. Taiar, V. Gremeaux-Bader, and K. Aminian, 2020. 191-197.

[12] Yang, X. and Liu, Z., (2005). Using Satellite Imagery and GIS for land‐Use and Land‐Cover Change Mapping in an Estuarine Watershed. *International Journal of Remote Sensing*, Vol. 26(23), 5275-5296, https://doi.org /10.1080/01431160500219224.

[13] Phiri, D., Simwanda, M., Salekin, S., Nyirenda, V. R., Murayama, Y. and Ranagalage, M., (2020). Sentinel-2 Data for Land Cover/Use Mapping: A Review. *Remote Sensing*, Vol. 12(14). https://doi.org/10.3390/rs12142291.

[14] Zheng, H., Du, P., Chen, J., Xia, J., Li, E., Xu, Z., Li, X., and Yokoya, N., (2017). Performance Evaluation of Downscaling Sentinel-2 Imagery for Land Use and Land Cover Classification by Spectral-Spatial Features. *Remote Sensing*, Vol. 9(12). https://doi.org/10.3390/rs9121274.

[15] Mutanga, O. and Kumar, L., (2019). Google Earth Engine Applications. *Remote Sensing*, Vol. 11(5). https://doi.org/10.3390/rs11050591.

[16] Zhao, Q., Yu, L., Li, X., Peng, D., Zhang, Y. and Gong, P., (2021). Progress and Trends in the Application of Google Earth and Google Earth Engine. *Remote Sensing*, Vol. 13(18). https://doi. org/10.3390/rs13183778.

[17] Jin, Z., Azzari, G., You, C., Di Tommaso, S., Aston, S., Burke, M. and Lobell, D. B., (2019). Smallholder Maize Area and Yield Mapping at National Scales with Google Earth Engine. *Remote Sensing of Environment*, Vol. 228, 115-128, https://doi.org/10.1016/j.rse.2019.04.016.

[18] Deng, Y., Jiang, W., Tang, Z., Ling, Z., and Wu, Z., (2019). Long-Term Changes of Open-Surface Water Bodies in the Yangtze River Basin Based on the Google Earth Engine Cloud Platform. *Remote Sensing*, Vol. 11(19). https://doi.org/ 10.3390/rs11192213.

[19] Xie, S., Liu, L., Zhang, X., Yang, J., Chen, X. and Gao, Y., (2019). Automatic Land-Cover Mapping Using Landsat Time-Series Data Based on Google Earth Engine. *Remote Sensing*, Vol. 11(24). https://doi.org/10.3390/rs11243023.

[20] Singha, M., Dong, J., Sarmah, S., You, N., Zhou, Y., Zhang, G., Doughty, R. and Xiao, X., (2020). Identifying Floods and Flood-Affected Paddy Rice Fields in Bangladesh Based on Sentinel-1 Imagery and Google Earth Engine. *ISPRS Journal of Photogrammetry and Remote Sensing*, Vol. 166, 278-293, https://doi.org/10. 1016/j.ispr sjprs.2020.06.011.

[21] Banerjee, A., Chen, R., Meadows, M. E., Sengupta, D., Pathak, S., Xia, Z. and Mal, S., (2021). Tracking 21st Century Climate Dynamics of the Third Pole: An Analysis of Topo-Climate Impacts on Snow Cover in the Central Himalaya Using Google Earth Engine. *International Journal of Applied Earth Observation and Geoinformation*, Vol. 103. https://doi.org/10.10 16/j.jag.2021.102490.

[22] Wang, W., Samat, A., Ge, Y., Ma, L., Tuheti, A., Zou, S. and Abuduwaili, J., (2020). Quantitative Soil Wind Erosion Potential Mapping for Central Asia Using the Google Earth Engine Platform. *Remote Sensing*, Vol. 12(20). https://doi.org/ 10.3390/rs12203430.

[23] Brovelli, M. A., Sun, Y. and Yordanov, V., (2020). Monitoring Forest Change in the Amazon Using Multi-Temporal Remote Sensing Data and Machine Learning Classification on Google Earth Engine. *ISPRS International Journal of Geo-Information*, Vol. 9(10). https:// doi.org/10.3390/ ijgi9100580.

[24] Hird, J. N., DeLancey, E. R., McDermid, G. J. and Kariyeva, J., (2017). Google Earth Engine, Open-Access Satellite Data, and Machine Learning in Support of Large-Area Probabilistic Wetland Mapping. *Remote Sensing*, Vol. 9(12). https://doi.org/10.3390/rs9121315.

[25] Keshtkar, H. and Voigt, W., (2015). A Spatiotemporal Analysis of Landscape Change Using an Integrated Markov Chain and Cellular automata Models. *Modeling Earth Systems and Environment*, Vol. 2(1). https://doi.org/10.1007/ s40808-015-0068-4.

[26] Wijitkosum, S. and Sriburi, T., (2019). Fuzzy AHP Integrated with GIS Analyses for Drought Risk Assessment: A Case Study from Upper Phetchaburi River Basin, Thailand. *Water*, Vol. 11(5). https://doi.org/10.3390/w11050939.

[27] Muller-Wilm, U., Louis, J., Richter, R., Gascon, F. and Niezette, M., (2013). Sentinel-2 Level 2A Prototype Processor: Architecture, Algorithms and First Results. *Proceedings of the ESA Living Planet Symposium, Edinburgh, UK*. 9-13.

[28] Louis, J., Pflug, B., Main-Knorn, M., Debaecker, V., Mueller-Wilm, U., Iannone, R. Q., Cadau, E. G., Boccia, V. and Gascon, F., (2019). Sentinel-2 Global Surface Reflectance Level-2A Product Generated with Sen2Cor. *IGARSS 2019-2019 IEEE International Geoscience and Remote Sensing Symposium*, 85 22-8525.

[29] Skakun, S., Skakun, S., Wevers, J., Brockmann, C., Doxani, G., Aleksandrov, M., Batič, M., Frantz, D., Gascon, F., Gómez-Chova, L., Hagolle, O., López-Puigdollers, D., Louis, J., Lubej, M., Mateo-García, G., Osman, J., Peressutti, D., Pflug, B., Puc, J., Richter, R., Roger, J., Scaramuzza, P., Vermote, E., Vesel, N., Zupanc, A. and Žust, L., (2022). Cloud Mask Intercomparison eXercise (CMIX): An Evaluation of Cloud Masking Algorithms for Landsat 8 and Sentinel-2. *Remote Sensing of Environment*, Vol. 274, https://doi.org/10.1016/ j.rse.2022.112990.

[30] Bordt, M., (2015). Advancing Environmental-Economic Accounting Concept Note on Global Land Cover for Policy Needs: Supporting SDG Monitoring and Ecosystem Accounting. *GEO-XII Plenary (Land Cover Side Event). Mexico City*, 2015.

[31] Prasai, R., Schwertner, T. W., Mainali, K., Mathewson, H., Kafley, H., Thapa, S., Adhikari, D., Medley, P. and Drake, J., (2021). Application of Google Earth Engine Python API and NAIP Imagery for Land Use and Land Cover Classification: A Case Study in Florida, USA. *Ecological Informatics*, Vol. 66, https:// doi.org/10.1016/j.ecoinf.2021.101474.

[32] Phan, T. N., Kuch, V. and Lehnert, L. W., (2020). Land Cover Classification using Google Earth Engine and Random Forest Classifier—The Role of Image Composition. *Remote Sensing*, Vol. 12(15), https://doi.org/10.3390/rs 12152411.

[33] Un and Desa, (2014). *System of Environmental-Economic Accounting 2012*, New York: United Nations Publications.

[34] Congalton, R. G., (1991). A Review of Assessing the Accuracy of Classifications of Remotely Sensed Data. *Remote Sensing of Environment*, Vol. 37(1), 35-46. https://doi.org /10.1016/0034-4257(91)90048-B.

[35] Koko, A. F., Yue, W., Abubakar, G. A., Hamed, R. and Alabsi, A. A. N., (2020). Monitoring and Predicting Spatio-Temporal Land Use/Land Cover Changes in Zaria City, Nigeria, through an Integrated Cellular Automata and Markov Chain Model (CA-Markov). *Sustainability*, Vol. 12(24), https://doi. org/10.3390/su122410452.

[36] Hamad, R., Balzter, H. and Kolo, K., (2018). Predicting Land Use/Land Cover Changes Using a CA-Markov Model under Two Different Scenarios. *Sustainability*, Vol. 10(10), https://doi .org/10.3390/su10103421.

[37] Sang, L., Zhang, C., Yang, J., Zhu, D. and Yun, W., (2011). Simulation of Land Use Spatial Pattern of Towns and Villages Based on CA–Markov Model. *Mathematical and Computer Modelling*, Vol. 54(3), 938-943. https://doi.org/ 10.1016/j.mcm.2010.11.019.

[38] Losiri, C., Nagai, M., Ninsawat, S. and Shrestha, R. P., (2016). Modeling Urban Expansion in Bangkok Metropolitan Region Using Demographic–Economic Data through Cellular Automata-Markov Chain and Multi-Layer Perceptron-Markov Chain Models. *Sustainability*, Vol. 8(7). https://doi.org/10.3390 /su8070686.

[39] Land Development Department (LDD), (2020). *The Appropriate Agricultural Extension Guidelines According to the Agricultural Map, Agri-map: Samut Songkhram*. BKK: LDD, [E-book] Available: http://www.ldd.go.th/Agri-Map /Data/C/skm.pdf

[40] TAT Newsroom, (2021). *Phetchaburi Honoured with UNESCO Creative City of Gastronomy Status*. Available: https://www. tatnews.org/ 2021/11/phetchaburi-honoured-with -unesco-creative-city-of-gastronomy-status/